

Spectral functions of isoscalar scalar and isovector electromagnetic form factors of the nucleon at two-loop order

N. Kaiser

Physik Department T39, Technische Universität München, D-85747 Garching, Germany

Abstract

We calculate the imaginary parts of the isoscalar scalar and isovector electromagnetic form factors of the nucleon up to two-loop order in chiral perturbation theory. Particular attention is paid on the correct behavior of $\text{Im } \sigma_N(t)$ and $\text{Im } G_{E,M}^V(t)$ at the two-pion threshold $t_0 = 4m_\pi^2$ in connection with the non-relativistic $1/M$ -expansion. We recover the well-known strong enhancement near threshold originating from the nearby anomalous singularity at $t_c = 4m_\pi^2 - m_\pi^4/M^2 = 3.98m_\pi^2$. In the case of the scalar spectral function $\text{Im } \sigma_N(t)$ one finds a significant improvement in comparison to the lowest order one-loop result. Higher order $\pi\pi$ -rescattering effects are however still necessary to close a remaining 20%-gap to the empirical scalar spectral function. The isovector electric and magnetic spectral functions $\text{Im } G_{E,M}^V(t)$ get additionally enhanced near threshold by the two-pion-loop contributions. After supplementing their two-loop results by a phenomenological ρ -meson exchange term one can reproduce the empirical isovector electric and magnetic spectral functions fairly well.

PACS: 12.38.Bx, 12.39.Fe, 13.40.Gp.

The structure of the nucleon as probed in elastic electron-nucleon scattering is encoded in four form factors $G_{E,M}^{S,V}(t)$ (with t the squared momentum transfer). The understanding of these form factors is of importance for any theory or model of the strong interactions. Abundant data on the electromagnetic form factors of the nucleon exist over a large range of momentum transfers, $0 < \sqrt{-t} < 6 \text{ GeV}$. Dispersion theory is a tool to interpret these data in a largely model-independent fashion. Each electromagnetic form factor $G_{E,M}^{S,V}(t)$ can be written in terms of an unsubtracted dispersion relation and their imaginary parts are often modeled by a few vector meson poles. This procedure is based on the successful vector meson dominance hypothesis which states that the (virtual) photon couples to hadrons only via intermediate vector mesons. However, as pointed out already in 1959 by Fulco and Frazer [1] such an approach is not in conformity with general constraints from unitarity and analyticity. In particular, the singularity structure of the triangle diagram (left graph in Fig. 1) is not respected at all when using only vector meson poles. As a consequence of a nearby logarithmic singularity at $t_c = 4m_\pi^2 - m_\pi^4/M^2$ (on the second Riemann-sheet) the low-mass two-pion continuum has a very pronounced effect on the isovector electric and magnetic spectral functions $\text{Im } G_{E,M}^V(t)$ on the left wing of the $\rho(770)$ -resonance. This becomes particularly visible in the isovector mean square radii of the nucleon. The effect was quantified by Höhler and Pietarinen [2] in their work on the nucleon electromagnetic form factors based on $\pi\pi \rightarrow \bar{N}N$ partial wave amplitudes. The dispersion relation analysis of the nucleon electromagnetic form factors was recently refined by the Bonn-Mainz group [3, 4] accounting for new electron scattering data and the high-energy constraints from perturbative QCD.

The first one-loop calculation of the isovector electromagnetic form factors has been performed in ref.[5] using the fully relativistic version of baryon chiral perturbation theory. The

correct analytical structure naturally emerged in this calculation and thus the strong enhancement near the two-pion threshold. In the framework of heavy baryon chiral perturbation theory next-to-leading order one-loop results for the isovector electric and magnetic spectral functions $\text{Im} G_{E,M}^V(t)$ have been given in ref.[6]. To that order a formally incorrect threshold behavior, not following the required p-wave phase space $\text{Im} G_{E,M}^V(t) \sim (t - 4m_\pi^2)^{3/2}$, has been obtained. This deviation is a consequence of the coalescence of the normal threshold $t_0 = 4m_\pi^2$ and the anomalous threshold $t_c = 4m_\pi^2 - m_\pi^4/M^2$ in the heavy nucleon limit $M \rightarrow \infty$. In that paper [6] also the isoscalar electric and magnetic spectral functions $\text{Im} G_{E,M}^S(t)$ (starting at two-loop order) have been computed. It has been shown that no substantial contribution arises from the three-pion continuum below the narrow $\omega(782)$ -resonance.

The purpose of this paper is to present results for the isovector electromagnetic spectral functions up to two-loop order in chiral perturbation theory paying special attention on the correct threshold behavior. We will include in our discussion also the isoscalar scalar form factor of the nucleon. Although not directly measurable this form factor $\sigma_N(t)$ is very interesting since it quantifies explicit chiral symmetry breaking effects in the nucleon ($\sigma_N(0) = \hat{m} \partial M / \partial \hat{m}$ is the celebrated pion-nucleon sigma-term). Moreover, its spectral function $\text{Im} \sigma_N(t)$ is completely dominated by the low-mass two-pion continuum due to the abovementioned threshold enhancement effect with no visible scalar resonance structures (see Fig. 4 in ref.[7]).

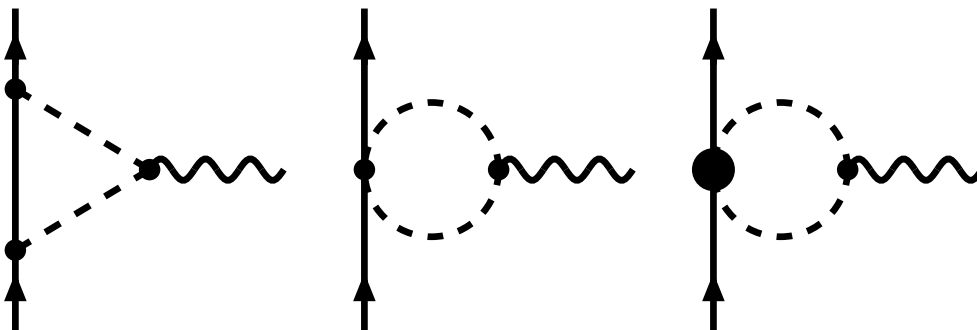


Fig.1: One-loop diagrams contributing to the imaginary parts of the isoscalar scalar and isovector electromagnetic form factors of the nucleon. Dashed and solid lines denote pions and nucleons, respectively. The wiggly line represents the external scalar or vector source. The heavy dot symbolizes the second-order chiral $\pi\pi NN$ -contact vertex proportional to the low-energy constants $c_{1,2,3,4}$. The combinatoric factor of the last two diagrams is $1/2$.

Let us begin with recalling the basic definition of the isoscalar scalar form factor $\sigma_N(t)$ of the nucleon:

$$\langle N(p') | \hat{m} \bar{q} q | N(p) \rangle = \sigma_N(t) \bar{u}(p') u(p). \quad (1)$$

Here, $\hat{m} = (m_u + m_d)/2$ denotes the average light quark mass, $t = (p' - p)^2$ is the Lorentz-invariant squared momentum transfer and $u(p)$ stands for a Dirac spinor. Similarly, the matrix element of the isovector vector current defines the isovector Dirac and Pauli form factors:

$$\langle N(p') | \bar{q} \gamma^\mu \tau_a q | N(p) \rangle = \bar{u}(p') \left[\gamma^\mu F_1^V(t) + \frac{i\sigma^{\mu\nu}}{2M} (p' - p)_\nu F_2^V(t) \right] \tau_a u(p), \quad (2)$$

where $M = 938.27 \text{ MeV}$ denotes the proton mass. In what follows, we will work with other linear combinations of $F_{1,2}^V(t)$, the isovector electric and magnetic (Sachs) form factors:

$$G_E^V(t) = F_1^V(t) + \frac{t}{4M^2} F_2^V(t), \quad G_E^V(0) = \frac{1}{2}, \quad (3)$$

$$G_M^V(t) = F_1^V(t) + F_2^V(t), \quad G_M^V(0) = \frac{\mu_p - \mu_n}{2} = 2.353, \quad (4)$$

which obey at $t = 0$ the normalization conditions written in eqs.(3,4). As usual, $\mu_p = 2.793$ and $\mu_n = -1.913$ denote the proton and neutron magnetic moments (in units of nuclear magnetons). In the complex t -plane the form factors $\sigma_N(t)$ and $G_{E,M}^V(t)$ have a right hand cut along the positive real axis starting at $t_0 = 4m_\pi^2$ related to the opening of the two-pion threshold. The imaginary parts $\text{Im} \sigma_N(t + i0^+)$ and $\text{Im} G_{E,M}^V(t + i0^+)$ of these nucleon form factors (equal to the half discontinuities across the cut) are also called their spectral functions.

The contributions to the spectral functions $\text{Im} \sigma_N(t)$ and $\text{Im} G_{E,M}^V(t)$ calculated up to two-loop order in chiral perturbation theory can be grouped into four different classes. The first class of contributions comes from the one-loop diagrams with leading order relativistic πN -interaction vertices and propagators (represented by the first and second diagram in Fig. 1). For these one-loop graphs we can take the fully relativistic expressions given in ref.[5] and expand them in inverse powers of the large nucleon mass M up to order $\mathcal{O}(M^{-2})$. This way one gets for the imaginary part of the isoscalar scalar form factor of the nucleon:

$$\text{Im} \sigma_N(t) = \frac{3g_A^2 m_\pi^2}{64\pi f_\pi^2 \sqrt{t}} \left\{ (t - 2m_\pi^2) A(t) \left[1 + \frac{3t}{8M^2} \right] - \frac{Qt}{2M} \right\}, \quad (5)$$

with the auxiliary functions:

$$A(t) = \arctan \frac{Q\sqrt{4M^2 - t}}{t - 2m_\pi^2}, \quad Q = \sqrt{t - 4m_\pi^2}. \quad (6)$$

The same procedure gives for the imaginary parts of the isovector electric and magnetic form factors of the nucleon:

$$\begin{aligned} \text{Im} G_E^V(t) &= \frac{1}{64\pi f_\pi^2 \sqrt{t}} \left\{ \frac{Q}{3} \left[g_A^2 (5t - 8m_\pi^2) + Q^2 \right] \right. \\ &\quad \left. - \frac{g_A^2}{M} (t - 2m_\pi^2)^2 A(t) \left[1 + \frac{3t}{8M^2} \right] + \frac{g_A^2 Q t}{2M^2} (t - 2m_\pi^2) \right\}, \end{aligned} \quad (7)$$

$$\begin{aligned} \text{Im} G_M^V(t) &= \frac{M}{32\pi f_\pi^2 \sqrt{t}} \left\{ g_A^2 Q^2 A(t) + \frac{Q}{6M} \left[g_A^2 (10m_\pi^2 - 4t) + Q^2 \right] \right. \\ &\quad \left. + \frac{g_A^2}{8M^2} (3t^2 - 12tm_\pi^2 + 8m_\pi^4) A(t) \right\}. \end{aligned} \quad (8)$$

It is important to note that the expressions in eqs.(5,7,8) possess the correct threshold behavior, namely $\text{Im} \sigma_N(t) \sim \sqrt{t - 4m_\pi^2}$ and $\text{Im} G_{E,M}^V(t) \sim (t - 4m_\pi^2)^{3/2}$. In order to achieve this property in all three cases a subleading term proportional to M^{-3} had to be kept in the isovector electric spectral function $\text{Im} G_E^V(t)$. One easily verifies that the coefficients of $Q = \sqrt{t - 4m_\pi^2}$ appearing in the threshold expansion of $\text{Im} G_{E,M}^V(t)$ vanish to the respective order in the $1/M$ -expansion. The crucial point about the representations eqs.(5,7,8) is not to further expand the function $A(t)$ in powers of $1/M$ as it is done (implicitly) in heavy baryon chiral perturbation theory [6]. In fact this function $A(t)$ incorporates the anomalous (logarithmic) singularity at $t_c = 4m_\pi^2 - m_\pi^4/M^2$, determined as that t -value where the argument of the arctangent-function becomes equal to $\pm i$. As a matter of fact the $1/M$ -expansion of the function $A(t)$ would destroy the correct analytical structure and moreover generate singular terms of the form Q^{-n} . From the point of view of chiral power counting the function $A(t)$

resumes an infinite string of terms starting at zeroth order. We note aside that the one-loop calculation of ref.[8] employing a so-called infrared regularization scheme gives naturally the correct threshold behavior of $\text{Im} G_{E,M}^V(t)$ since there the spectral functions are identical to those of the fully relativistic framework [5].

The next class of contributions is given by the one-loop diagrams with one second order chiral $\pi\pi NN$ -contact vertex proportional to the low-energy constants $c_{1,2,3,4}$ [9]. We obtain from the last diagram in Fig. 1 the following contributions to the spectral functions:

$$\text{Im} \sigma_N(t) = \frac{m_\pi^2 Q}{64\pi f_\pi^2 \sqrt{t}} \left[4m_\pi^2 (c_2 + 3c_3 - 6c_1) - t(c_2 + 6c_3) \right], \quad (9)$$

$$\text{Im} G_E^V(t) = \frac{c_4 Q^3 \sqrt{t}}{192\pi M f_\pi^2}, \quad \text{Im} G_M^V(t) = \frac{c_4 M Q^3}{48\pi f_\pi^2 \sqrt{t}}, \quad (10)$$

where we have included also the first relativistic $1/M$ -correction (as far as it does not vanish). The separation of the $\pi\pi NN$ -contact vertex into an isoscalar part proportional to $c_{1,2,3}$ and an isovector part proportional to c_4 is obvious from eqs.(9,10). The same c_4 -contribution to $\text{Im} G_M^V(t)$ has been written down first in eq.(10) of ref.[6].

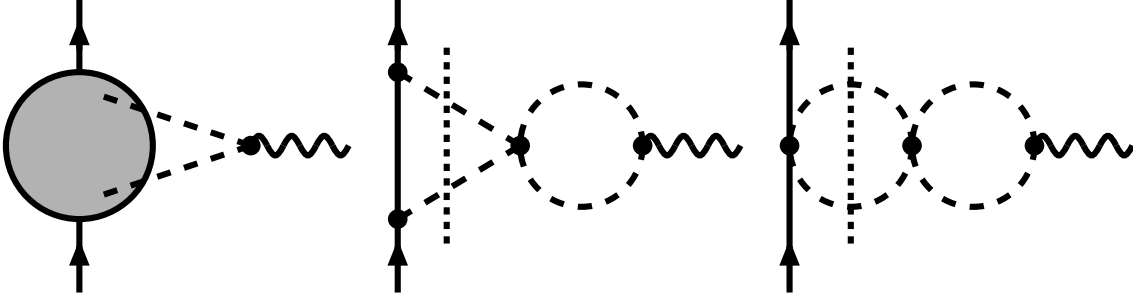


Fig.2: Two-loop diagrams contributing to the imaginary parts of the isoscalar scalar and isovector electromagnetic form factors of the nucleon. The grey disk symbolizes all one-loop diagrams of elastic πN -scattering. The combinatoric factor of the first two diagrams is $1/2$. The vertical dotted line indicates that cut which splits off the (one-loop) scalar or charge form factor of the pion from these factorizable diagrams.

Now we turn to the two-loop diagrams. These are symbolically represented by the left graph in Fig. 2. The grey disk should be interpreted such that it includes all one-loop diagrams of elastic πN -scattering. Exploiting unitarity the imaginary parts $\text{Im} \sigma_N(t)$ and $\text{Im} G_{E,M}^V(t)$ can be calculated from these two-loop diagrams as integrals of the product of *scalar/vector source* $\rightarrow 2\pi$ and $2\pi \rightarrow \bar{N}N$ transition amplitude over the Lorentz-invariant two-pion phase space. When evaluated in the $\pi\pi$ center-of-mass frame the pertinent two-pion phase space integrals become proportional to simple angular integrals $\int_{-1}^1 dx$. Consider now that cut which splits a two-loop diagram into a tree-level *source* $\rightarrow 2\pi$ coupling and a one-loop diagram of elastic πN -scattering. Putting together all such terms we find the following two-loop contribution to the imaginary part of the scalar form factor of the nucleon:

$$\begin{aligned} \text{Im} \sigma_N(t) = & \frac{3m_\pi^2}{\pi^2 (8f_\pi)^4} \left\{ \frac{4m_\pi^2}{\sqrt{t}} \left[g_A^4 (10m_\pi^2 - 4t) - m_\pi^2 \right] \ln \frac{\sqrt{t} + Q}{2m_\pi} \right. \\ & + Q \left[\left(\frac{1}{2} - g_A^4 \right) (t - 2m_\pi^2) + \frac{8g_A^4 m_\pi^2 (\sqrt{t} - 2m_\pi) (5\sqrt{t} + 8m_\pi)}{3(t + 2m_\pi \sqrt{t})} \right. \\ & \left. \left. + g_A^2 (m_\pi^2 - 2t) \left(\frac{4m_\pi}{\sqrt{t}} + \frac{2m_\pi^2 - t}{t} \ln \frac{\sqrt{t} + 2m_\pi}{\sqrt{t} - 2m_\pi} \right) \right] \right\}. \quad (11) \end{aligned}$$

This expression is identical to the 2π -phase space integral $3m_\pi^2(32\pi\sqrt{t})^{-1} \int_{-Q/2}^{Q/2} dk \operatorname{Re} g^+(ik, t)$ with $g^+(\omega, t)$ the isospin-even non-spin-flip one-loop πN -amplitude [9, 10]. The analogous contribution to the isovector electric spectral function reads:

$$\begin{aligned}
\operatorname{Im} G_E^V(t) &= \frac{g_A^4 m_\pi^2 (2m_\pi^2 - t)}{192\pi^3 f_\pi^4 \sqrt{t}} \int_0^{Q/2} dk \frac{\sqrt{m_\pi^2 + k^2}}{k} \ln \frac{k + \sqrt{m_\pi^2 + k^2}}{m_\pi} \\
&+ \frac{1}{9\pi^3 (4f_\pi)^4} \left\{ \frac{g_A^4 t}{20} (20m_\pi^2 - 7t) + \frac{g_A^2 Q^4}{4t} (8m_\pi^2 - 5t) + \frac{16m_\pi^6}{t} - 12m_\pi^4 + \frac{t^2}{5} \right\} \\
&\times \ln \frac{\sqrt{t} + Q}{2m_\pi} + \frac{Q}{(24\pi)^3 f_\pi^4 \sqrt{t}} \left\{ \frac{g_A^4}{100} (257t^2 + 2604m_\pi^2 t - 6368m_\pi^4) \right. \\
&+ \left. \frac{g_A^2}{4} Q^2 (13t - 48m_\pi^2) + \frac{1}{25} (684m_\pi^4 + 73m_\pi^2 t - 16t^2) \right\} \\
&+ \frac{Q^3}{480\pi f_\pi^2 \sqrt{t}} \left[10(\bar{d}_1 + \bar{d}_2)(2m_\pi^2 - t) - 3\bar{d}_3 Q^2 + 40\bar{d}_5 m_\pi^2 \right]. \tag{12}
\end{aligned}$$

The term in the last line originates from the third order scale-independent low-energy constants \bar{d}_j introduced in ref.[9] which subsume already chiral logarithms $\ln(m_\pi/\lambda)$. The remainder in eq.(12) is identical to the 2π -phase space integral $(8\pi\sqrt{t})^{-1} \int_{-Q/2}^{Q/2} dk \operatorname{Re} [-ik g^-(ik, t)]$ with $g^-(\omega, t)$ the isospin-odd non-spin-flip one-loop πN -amplitude [9, 10]. The analogous contribution to the isovector magnetic spectral function reads:

$$\begin{aligned}
\operatorname{Im} G_M^V(t) &= \frac{g_A^2 M}{\pi^2 (4f_\pi)^4 \sqrt{t}} \left\{ g_A^2 m_\pi^2 (5m_\pi^2 - t) \ln \frac{\sqrt{t} + Q}{2m_\pi} - Q^3 \frac{m_\pi}{6} \right. \\
&+ \left. \frac{Q^5}{24\sqrt{t}} \ln \frac{\sqrt{t} + 2m_\pi}{\sqrt{t} - 2m_\pi} + \frac{g_A^2 Q}{24} (30m_\pi^2 \sqrt{t} - 64m_\pi^3 - t^{3/2}) \right\}. \tag{13}
\end{aligned}$$

Again, this expression is identical to $M(32\pi\sqrt{t})^{-1} \int_{-Q/2}^{Q/2} dk (Q^2 - 4k^2) \operatorname{Re} h^-(ik, t)$ with $h^-(\omega, t)$ the isospin-odd spin-flip one-loop πN -amplitude [9, 10]. We emphasize the correct threshold behavior of the two-loop contributions: $\operatorname{Im} \sigma_N(t) \sim Q$ according to eq.(11) and $\operatorname{Im} G_{E,M}^V(t) \sim Q^3$ according to eqs.(12,13). In the latter two cases one easily verifies that the coefficients of Q vanish identically.

The full set of two-loop graphs contains the two factorizable diagrams exhibited in Fig. 2. Both cuts of the intermediate pion-pair generate a contribution to the imaginary parts, according to the rule: $\operatorname{Im}(z_1 z_2) = \operatorname{Re} z_1 \cdot \operatorname{Im} z_2 + \operatorname{Im} z_1 \cdot \operatorname{Re} z_2$. Only one term of this sum is accounted for in the expressions eqs.(11,12,13). The other term arises from that cut which splits off the one-loop scalar or charge form factor of the pion [11] (as symbolized by the vertical dotted line in Fig. 2). Naturally, the scalar form factor of the pion enters the scalar spectral function:

$$\operatorname{Im} \sigma_N(t) = \frac{g_A^2 m_\pi^2 (t - 2m_\pi^2)}{\pi^3 (4f_\pi)^4 \sqrt{t}} A(t) \left\{ 2\pi^2 f_\pi^2 \langle r_S^2 \rangle_\pi t + \frac{25t}{16} - \frac{3}{8} m_\pi^2 (1 + \bar{l}_3) + \frac{3Q}{4\sqrt{t}} (m_\pi^2 - 2t) \ln \frac{\sqrt{t} + Q}{2m_\pi} \right\}. \tag{14}$$

Here, $\langle r_S^2 \rangle_\pi$ denotes the mean square scalar radius of the pion. The low-energy constant $\bar{l}_3 \simeq 3$ [11] shows up in the one-loop representation of the pionic sigma-term: $\sigma_\pi(0) = \hat{m} \partial m_\pi^2 / \partial \hat{m} = m_\pi^2 + m_\pi^4 (1 - \bar{l}_3) / 32\pi^2 f_\pi^2 \simeq 0.99m_\pi^2$ [11]. On the other hand side, the (one-loop) pion charge form factor [11] enters the isovector electric and magnetic spectral functions:

$$\begin{aligned}
\operatorname{Im} G_E^V(t) &= \frac{1}{9\pi^3 (4f_\pi)^4 \sqrt{t}} \left\{ Q \left[g_A^2 (5t - 8m_\pi^2) + Q^2 \right] - \frac{3g_A^2}{M} (t - 2m_\pi^2)^2 A(t) \right\} \\
&\times \left\{ 2\pi^2 f_\pi^2 \langle r_{ch}^2 \rangle_\pi t + \frac{t}{3} - m_\pi^2 - \frac{Q^3}{4\sqrt{t}} \ln \frac{\sqrt{t} + Q}{2m_\pi} \right\}, \tag{15}
\end{aligned}$$

$$\text{Im } G_M^V(t) = \frac{g_A^2 M Q^2 A(t)}{3\pi^3 (4f_\pi)^4 \sqrt{t}} \left\{ (2\pi f_\pi)^2 \langle r_{ch}^2 \rangle_\pi t + \frac{2t}{3} - 2m_\pi^2 - \frac{Q^3}{2\sqrt{t}} \ln \frac{\sqrt{t} + Q}{2m_\pi} \right\}, \quad (16)$$

where $\langle r_{ch}^2 \rangle_\pi$ denotes the mean square charge radius of the pion. In order to guarantee the correct threshold behavior $\text{Im } G_E^V(t) \sim Q^3$ we have kept the first relativistic $1/M$ -correction (see eq.(7)) in the first factor of eq.(15).

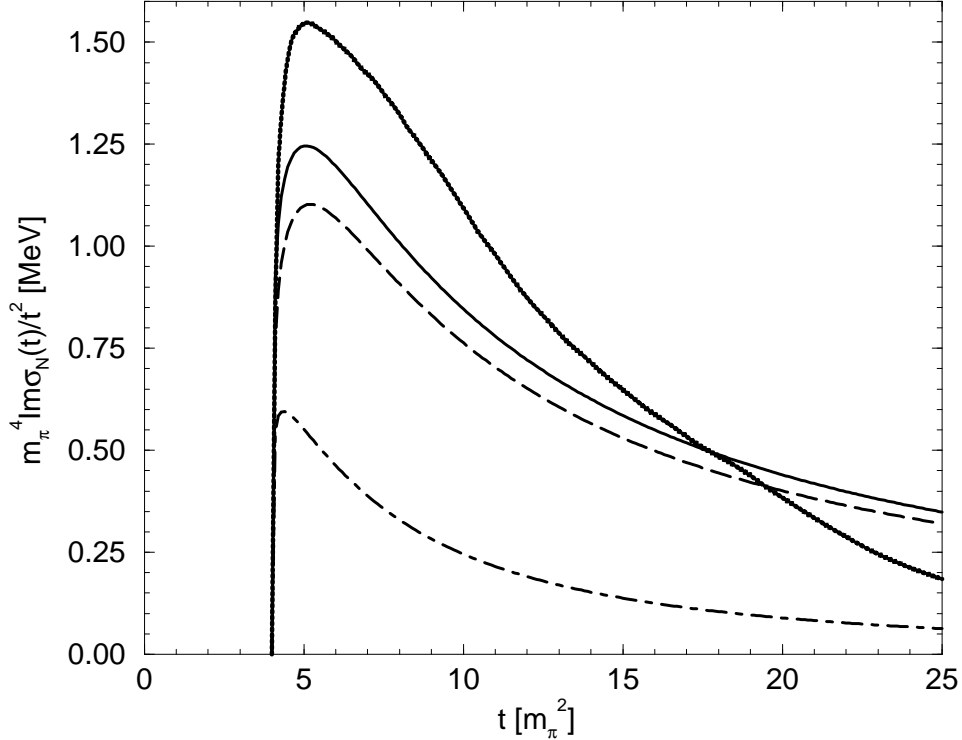


Fig.3: The spectral function $\text{Im } \sigma_N(t)$ of the isoscalar scalar form factor of the nucleon multiplied with m_π^4/t^2 . The dashed-dotted line gives the one-loop result eq.(5). The dashed line includes in addition the $c_{1,2,3}$ -term eq.(9) and the full line includes furthermore the two-loop contributions eqs.(11,14). The upper dotted line shows the empirical spectral function $m_\pi^4 \text{Im } \sigma_N(t)/t^2$ of ref.[7].

Let us add a remark on chiral power counting of the spectral functions. Counting the quantities \sqrt{t} , m_π and $Q = \sqrt{t - 4m_\pi^2}$ as small momenta one deduces that two-loop contributions to $\text{Im } \sigma_N(t)$, $\text{Im } G_E^V(t)$ and $\text{Im } G_M^V(t)$ are of fifth, fourth and third order in small momenta, respectively. In the latter two cases the electric/magnetic coupling of the (virtual) photon absorbs one/two powers of small momenta.

Let us now turn to numerical results. We use the parameters: $m_\pi = 139.57$ MeV (charged pion mass), $f_\pi = 92.4$ MeV (pion decay constant) and $g_A = 1.3$ (equivalent to a πN -coupling constant $g_{\pi N} = g_A M / f_\pi = 13.2$ [13]). For the second and third order low-energy constants c_i and \bar{d}_j we choose the average values of three fits to πN -phase shift solutions given in ref.[9]: $c_1 = -1.4$ GeV $^{-1}$, $c_2 = 3.2$ GeV $^{-1}$, $c_3 = -6.0$ GeV $^{-1}$, $c_4 = 3.5$ GeV $^{-1}$, $\bar{d}_1 + \bar{d}_2 = 3.0$ GeV $^{-2}$, $\bar{d}_3 = -3.0$ GeV $^{-2}$ and $\bar{d}_5 = 0.1$ GeV $^{-2}$. Most of these values are compatible with the low-energy constants c_i and \bar{d}_j obtained in ref.[12] in a one-loop analysis of πN -scattering inside the Mandelstam triangle. The mean square charge radius of the pion is accurately measured in elastic pion-electron scattering: $\langle r_{ch}^2 \rangle_\pi = (0.44 \pm 0.01)$ fm 2 [14]. A value compatible with that has been found in ref.[15] in a two-loop analysis of the low-energy $\pi^- e^-$ -scattering data.

An improved determination of the mean square scalar radius of the pion has recently been given in ref.[16]: $\langle r_S^2 \rangle_\pi = (0.61 \pm 0.04) \text{ fm}^2$. We use throughout the central values of these empirical pion mean square radii.

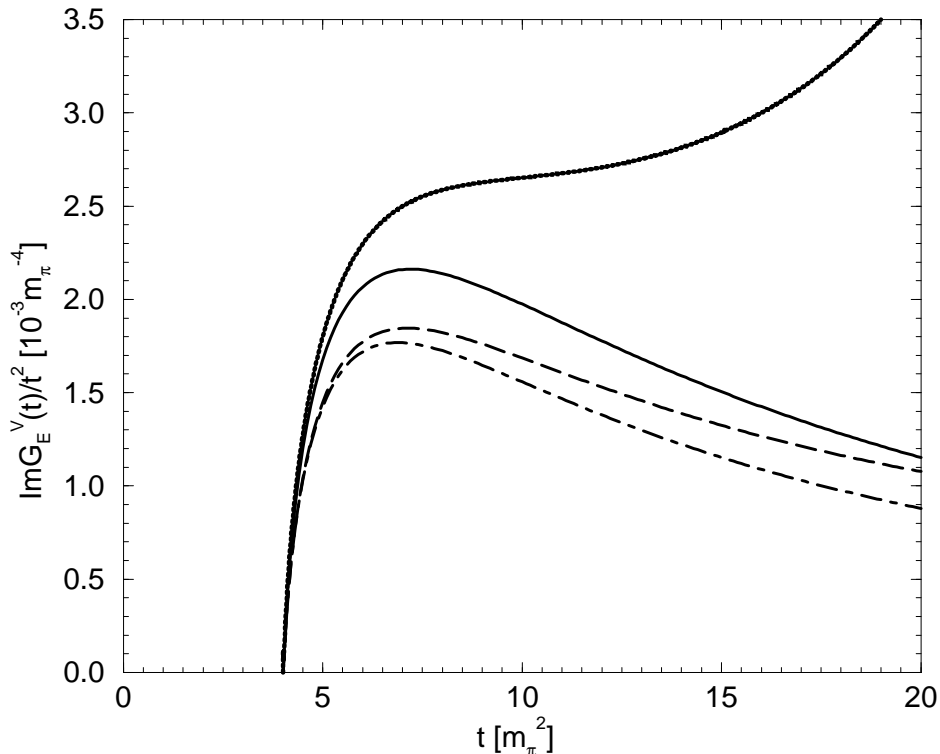


Fig.4: The spectral function $\text{Im}G_E^V(t)$ of the isovector electric form factor of the nucleon divided by t^2 . The dashed-dotted line gives the one-loop result eq.(7). The dashed line includes in addition the c_4/M -term eq.(10) and the full line includes furthermore the two-loop contributions eqs.(12,15). The upper dotted line shows the empirical spectral function $\text{Im}G_E^V(t)/t^2$ of ref.[2].

In Fig. 3 we show the spectral function $\text{Im}\sigma_N(t)$ of the isoscalar scalar form factor of the nucleon multiplied with a weighting factor m_π^4/t^2 . The dashed-dotted line gives the one-loop result eq.(5). The dashed line includes in addition the $c_{1,2,3}$ -term eq.(9) and the full line includes furthermore the two-loop contributions eqs.(11,14). The upper dotted line shows the empirical isoscalar scalar spectral function $m_\pi^4 \text{Im}\sigma_N(t)/t^2$ of ref.[7]. It has been determined on the basis of the $\pi\pi \rightarrow \bar{N}N$ s-wave amplitude $f_+^0(t)$ [2] and $\pi\pi$ -scattering data tied together with Roy-equations etc. (see eq.(3) in ref.[7]). One observes a substantial improvement when including the next-to-leading order $c_{1,2,3}$ -term and the two-loop contributions. The major effect comes evidently from the large isoscalar $\pi\pi NN$ -contact couplings, in particular from c_3 . The height of the peak at $t \simeq 5m_\pi^2$ is however still underestimated by about 20% in two-loop approximation. Higher order $\pi\pi$ -rescattering effects etc. are necessary in order to close this remaining gap. Given the pattern in Fig. 3 one can expect significant effects (in the right direction) already from the two-loop diagrams with one vertex proportional to the (numerically large) second order low-energy constants $c_{1,2,3,4}$. Note that a complete calculation of elastic πN -scattering to chiral order four which includes the pertinent one-loop diagrams with one $c_{1,2,3,4}$ -vertex has been recently performed in ref.[17]. For comparison, similar deficiencies of the two-loop approximation of chiral perturbation theory have been observed in ref.[18] for the imaginary parts of the pion scalar and charge form factors.

Next, we show in Fig. 4 the spectral function $\text{Im} G_E^V(t)$ of the isovector electric form factor of the nucleon weighted with $1/t^2$. The dashed-dotted line gives the one-loop result eq.(7). The dashed line includes in addition the c_4/M -term in eq.(10) and the full line includes furthermore the two-loop contributions eqs.(12,15). The upper dotted line corresponds to the empirical isovector electric spectral function $\text{Im} G_E^V(t)/t^2$ of ref.[2]. Modulo a kinematical factor $Q^3/8M\sqrt{t}$ it is determined by the product of the $\pi\pi \rightarrow \bar{N}N$ p-wave amplitude $f_+^1(t)$ [2] and the (time-like) pion charge form factor measured in the reaction $e^+e^- \rightarrow \pi^+\pi^-$ (see eq.(7) in ref.[6]). In the case of the isovector electric spectral function the two-loop contribution is considerably larger than the c_4/M -term (of the same chiral order). The peak at low $\pi\pi$ -invariant masses, $t \simeq 7m_\pi^2$, gets effectively enhanced by a factor of about 1.2 by this additional πN - and $\pi\pi$ -rescattering dynamics. The other prominent feature of the empirical isovector electric spectral function $\text{Im} G_E^V(t)$, namely its rise to the $\rho(770)$ -resonance, is clearly absent in (chiral) perturbation theory.

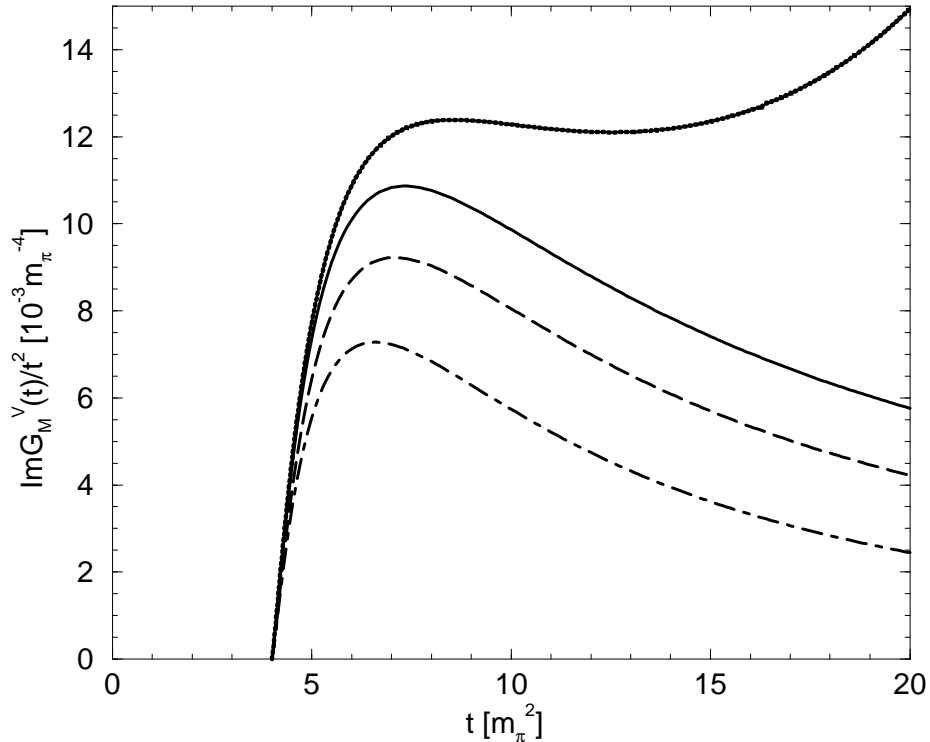


Fig.5: The spectral function $\text{Im} G_M^V(t)$ of the isovector magnetic form factor of the nucleon divided by t^2 . The dashed-dotted line gives the one-loop result eq.(8). The dashed line includes in addition the c_4 -term eq.(10) and the full line includes furthermore the two-loop contributions eqs.(13,16). The upper dotted line shows the empirical spectral function $\text{Im} G_E^V(t)/t^2$ of ref.[2].

Furthermore, we show in Fig. 5 the spectral function $\text{Im} G_M^V(t)$ of the isovector magnetic form factor of the nucleon weighted with $1/t^2$. The dashed-dotted line gives the one-loop result eq.(8). The dashed line includes in addition the c_4 -term in eq.(10) and the full line includes furthermore the two-loop contributions eqs.(13,16). The upper dotted line corresponds to the empirical isovector magnetic spectral function $\text{Im} G_M^V(t)/t^2$ of ref.[2]. Modulo a kinematical factor $Q^3/8\sqrt{2t}$ it is determined by the product of the $\pi\pi \rightarrow \bar{N}N$ p-wave amplitude $f_-^1(t)$ and the (time-like) pion charge form factor (see again eq.(7) in ref.[6]). In the case of the isovector magnetic spectral function the two-loop contribution and the next-to-leading order c_4 -term are approximately equal in magnitude. Both together enhance the peak slightly above

threshold considerably by a factor of about 1.5. Again, the strong rise of the empirical isovector magnetic spectral function $\text{Im} G_M^V(t)$ to the $\rho(770)$ -resonance cannot be reproduced in (chiral) perturbation theory.

For a more complete description of the dynamics governing the empirical isovector electromagnetic spectral functions the introduction of an explicit $\rho(770)$ -resonance is indispensable. For that reason we add a phenomenological ρ -meson exchange contribution of the simple form:

$$\text{Im} G_{E,M}^V(t) = \frac{b_{E,M} m_\rho^2 \sqrt{t} \Gamma_\rho(t)}{(m_\rho^2 - t)^2 + t \Gamma_\rho^2(t)}, \quad \Gamma_\rho(t) = \frac{g_{\rho\pi}^2 Q^3}{48\pi t}, \quad (17)$$

which of course includes the proper energy-dependent $\rho \rightarrow 2\pi$ decay width $\Gamma_\rho(t)$. We take the value $m_\rho = 769.3 \text{ MeV}$ [19] for the ρ -meson mass and coupling constant $g_{\rho\pi} = 6.03$ is determined from the empirical decay width $\Gamma_\rho(m_\rho^2) = 150.2 \text{ MeV}$ [19]. Furthermore, $b_E = 1.0$ and $b_M = 3.5$ are numerical parameters which we have adjusted to the height of the $\rho(770)$ -resonance peak (at $t \simeq 28m_\pi^2$) of the empirical isovector electric and magnetic spectral functions $\text{Im} G_{E,M}^V(t)/t^2$.

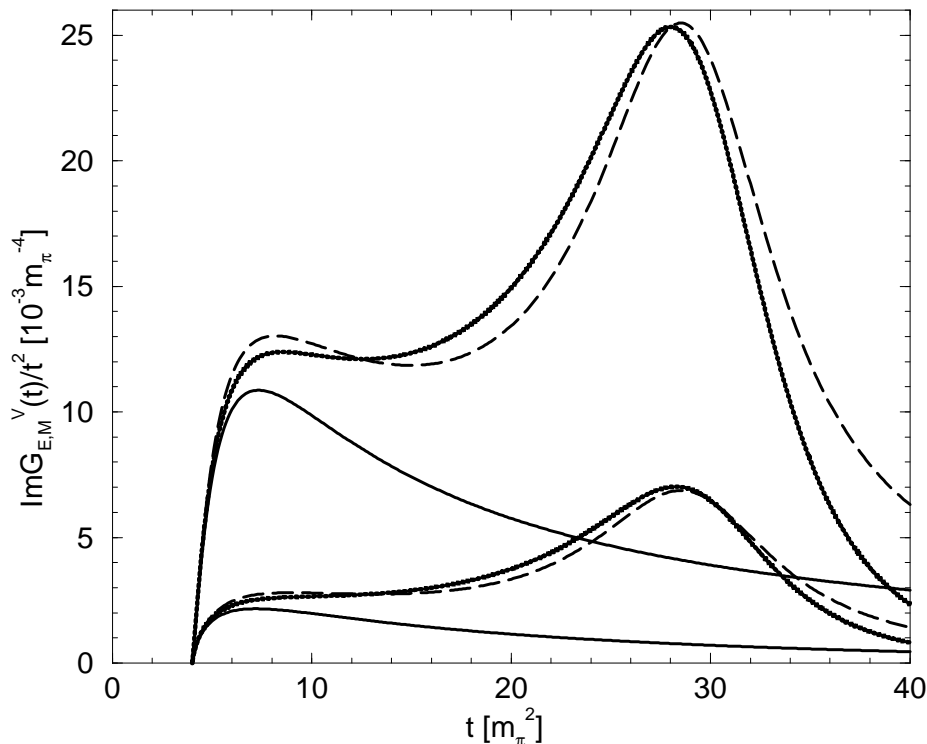


Fig.6: Spectral functions of the isovector electric and magnetic form factor of the nucleon weighted with $1/t^2$. Shown are $\text{Im} G_E^V(t)/t^2$ (lower three lines) and $\text{Im} G_M^V(t)/t^2$ (upper three lines). The full lines give the two-loop results of chiral perturbation theory and the dashed lines include in addition the phenomenological ρ -meson contribution eq.(17). The dotted curves correspond to the empirical spectral function $\text{Im} G_{E,M}^V(t)/t^2$ of ref.[2].

Finally, the lower (upper) lines in Fig.6 show the isovector electric (magnetic) spectral function weighted with $1/t^2$. The full lines give the respective two-loop result of chiral perturbation theory and the dashed lines include in addition the phenomenological ρ -meson exchange contribution eq.(17). One observes that the empirical isovector electric and magnetic spectral functions (dotted lines) can now be reproduced fairly well. The agreement is rather satisfactory for the electric one. In the case of the isovector magnetic spectral function $\text{Im} G_M^V(t)/t^2$

some overshooting and undershooting of the empirical values below and above $t \simeq 13m_\pi^2$ is visible in Fig. 6. This may point towards the relevance of higher order $\pi\pi$ -rescattering effects, or it may just result from the simplicity of the $\rho(770)$ -resonance parameterization eq.(17). In any case one should not overinterpret the small differences between the dashed and dotted lines in Fig. 6 since there may be a potential danger of double-counting when adding together perturbative chiral pion loops and a finite width $\rho(770)$ -meson exchange term (representing non-perturbative pion-dynamics).

In summary, we have calculated in this work the imaginary parts of the isoscalar scalar and isovector electromagnetic form factors of the nucleon up to two-loop order in chiral perturbation theory. We have performed the non-relativistic $1/M$ -expansion such that the correct threshold behavior, $\text{Im } \sigma_N(t) \sim \sqrt{t - 4m_\pi^2}$ and $\text{Im } G_{E,M}^V(t) \sim (t - 4m_\pi^2)^{3/2}$, is ensured. The two-loop contributions and the next-to-leading order $c_{1,2,3,4}$ -terms magnify the strong enhancement slightly above the two-pion threshold. Higher order $\pi\pi$ -rescattering effects etc. are still necessary to close a remaining 20%-gap to the empirical isoscalar scalar spectral function $\text{Im } \sigma_N(t)$ [7]. After adding a phenomenological $\rho(770)$ -meson exchange term to the respective two-loop results the empirical isovector electric and magnetic spectral functions $\text{Im } G_{E,M}^V(t)$ [2] can be reproduced fairly well.

I thank Ulf-G. Meißner for his tabulated values of the empirical isovector electromagnetic spectral functions $\text{Im } G_{E,M}^V(t)$ and for critical reading of the manuscript.

References

- [1] W.R. Frazer and J.R. Fulco, *Phys. Rev. Lett.* **2**, 365 (1959); *Phys. Rev.* **117**, 1609 (1960).
- [2] G. Höhler and E. Pietarinen, *Phys. Lett.* **B53**, 471 (1975); G. Höhler, Landolt-Börnstein, Vol.9b2, ed. H. Schopper, Springer-Verlag (1983), chapters 2.5.2 and 11.
- [3] P. Mergell, Ulf-G. Meißner and D. Drechsel, *Nucl. Phys.* **A596**, 367 (1996); and references therein.
- [4] H.W. Hammer, Ulf-G. Meißner and D. Drechsel, *Phys. Lett.* **B385**, 343 (1996).
- [5] J. Gasser, M.E. Sainio and A. Svarc, *Nucl. Phys.* **B307**, 779 (1988).
- [6] V. Bernard, N. Kaiser and Ulf-G. Meißner, *Nucl. Phys.* **A611**, 429 (1996).
- [7] J. Gasser, H. Leutwyler and M.E. Sainio, *Phys. Lett.* **B253**, 260 (1991); and references therein.
- [8] B. Kubis and Ulf-G. Meißner, *Nucl. Phys.* **A679**, 698 (2001).
- [9] N. Fettes, Ulf-G. Meißner and S. Steininger, *Nucl. Phys.* **A640**, 199 (1998).
- [10] V. Bernard, N. Kaiser and Ulf-G. Meißner, *Nucl. Phys.* **A615**, 483 (1997).
- [11] J. Gasser and H. Leutwyler, *Ann. Phys.* **158**, 142 (1984).
- [12] P. Büttiker and Ulf-G. Meißner, *Nucl. Phys.* **A668**, 97 (2000).
- [13] M.M. Pavan, R.A. Arndt, I.I. Strakovsky and R.L. Workman, *Phys. Scr.* **T87**, 65 (2000).
- [14] S.R. Amendolia et al., NA7 Collaboration, *Nucl. Phys.* **B277**, 168 (1986).
- [15] J. Bijnens and P. Talavera, *JHEP* **0203** (2002) 046.
- [16] G. Colangelo, J. Gasser and H. Leutwyler, *Nucl. Phys.* **B603**, 125 (2001); and references therein.
- [17] N. Fettes and Ulf-G. Meißner, *Nucl. Phys.* **A676**, 311 (2000).
- [18] J. Gasser and Ulf-G. Meißner, *Nucl. Phys.* **B357**, 90 (1991).
- [19] Review of Particle Properties, D.E. Groom et al., *Eur. Phys. J.* **C15**, 1 (2000).